Hindawi Publishing Corporation
Journal of Chemistry
Volume 2014, Article ID 679281, 10 pages
http://dx.doi.org/10.1155/2014/679281

Research Article

Monometallic Pd and Pt and Bimetallic Pd-Pt/Al_2O_3-TiO_2 for the HDS of DBT: Effect of the Pd and Pt Incorporation Method

Reynaldo Martínez Guerrero,[1] Agileo Hernández-Gordillo,[2] Víctor Santes,[2] Jorge Roberto Vargas García,[1] José Escobar,[3] Leonardo Díaz-García,[3] Lucía Díaz Barriga Arceo,[1] and Vicente Garibay Febles[3]

[1] *Departamento de Ingeniería Metalúrgica, ESIQIE-Instituto Politécnico Nacional, 07300 México, DF, Mexico*
[2] *Departamento de Biociencias e Ingeniería, CIIEMAD-Instituto Politécnico Nacional, 07340 México, DF, Mexico*
[3] *Instituto Mexicano del Petróleo, Eje Central 152, 07730 México, DF, Mexico*

Correspondence should be addressed to Víctor Santes; vsantes@ipn.mx

Received 15 August 2014; Accepted 30 October 2014; Published 26 November 2014

Academic Editor: Davut Avci

The effect of the preparation method of monometallic Pd and Pt and bimetallic Pd-Pt/Al_2O_3-TiO_2 catalysts on the hydrodesulfurization (HDS) of dibenzothiophene (DBT) was investigated in this study. The synthesis was accomplished using three methods: (A) impregnation, (B) metal organic chemical vapor deposition (MOCVD), and (C) impregnation-MOCVD. The bimetallic Pd-Pt catalyst prepared by the impregnation-MOCVD method was most active for the HDS of DBT compared to those prepared by the single impregnation or MOCVD method due to the synergetic effect between both noble metals. The greater selectivity toward biphenyl indicated that this bimetallic Pd-Pt catalyst preferentially removes sulfur via the direct desulfurization mechanism. However, the bimetallic Pd-Pt catalyst prepared using the single MOCVD method did not produce any cyclohexylbenzene, which is most likely associated with the hydrogenation/dehydrogenation sites.

1. Introduction

The hydrodesulfurization (HDS) of straight run gasoil (SRGO) is receiving considerable attention due to stringent environmental requirements, such as a lower sulfur content and the elimination of aromatic compounds in diesel fuel [1–4]. The different sulfur-containing compounds in SRGO include dibenzothiophene (DBT), 4-methyl-dibenzothiophene, and 4,6-dimethyl dibenzothiophene (46DMDBT) [5, 6]. The mechanisms for eliminating sulfur compounds follow two routes (i.e., direct desulfurization (DDS) and the hydrogenation (HYD)). However, the reactivity between DBT and 46DMDBT presents differences in terms of the preferential reaction pathways. In general, DBT is desulfurized via the DDS route while 46DMDBT is desulfurized via the HYD route [7, 8]. In this case, strong hydrogenating catalytic sites are preferable for the successful removal of refractory sulfur compounds, such as 46DMDT. Conventional supported Ni-Mo sulfide hydrotreating catalysts become active in the HYD route only at high pressure due to the thermodynamic limitation [9]. However, precious metals, such as Pd and Pt, have exhibited a higher hydrogenation ability at lower temperatures compared to metallic sulfides in hydrotreating catalysts. Unfortunately, monometallic Pd or Pt are easily poisoned by hydrogen sulfide. Therefore, their use as hydrogenation catalysts is only attractive when the feedstock is free of sulfur or when the sulfur-metal reaction is inhibited [10, 11]. Pd/Al_2O_3 catalysts are better than Pt/Al_2O_3 catalysts for the hydrodesulfurization of either DBT or 46DMDBT, which is due to the higher hydrogenation ability of palladium. Indeed, better hydrodesulfurization results have been observed with the use of bimetallic Pt-Pd/Al_2O_3 catalysts [12, 13]. The sulfur resistance of the noble metal catalysts has been increased using bimetallic Pd-Pt supported on different mixed oxides, such as zeolite, SiO_2-Al_2O_3, and amorphous SiO_2 [14–19]. Recently, Galindo and

de los Reyes [20] reported that monometallic Pd and Pt supported on Al_2O_3-TiO_2 exhibited higher HDS activity than those supported on Al_2O_3. In addition, Guofu et al. [21] reported that the integration of TiO_2 into Al_2O_3 facilitates the dispersion of supported Pt-Pd bimetallic particles, which leads to higher hydrodesulfurization activity and better stability.

For the synthesis of HDS catalysts, conventional wet impregnation has been the most frequently employed method for metal incorporation. However, this process requires several steps in the preparation and has several limitations to good metallic dispersion [22]. In this case, the metallic dispersion is strongly influenced by the metal precursors, temperature pretreatment, gas atmosphere, and other factors [23]. By contrast, the metal organic chemical vapor deposition (MOCVD) method has been extended to the preparation of noble metal supported catalysts in a single step. In this case, fine metallic particles can be highly dispersed on the support [24–26]. However, to our knowledge, there are no studies concerning the effect of bimetallic Pd-Pt catalysts prepared by single MOCVD or combined impregnation-MOCVD method in the HDS of DBT. Therefore, in this study, we report the effect of the integration method of a metallic active phase on the catalytic performance of monometallic Pd and Pt catalysts and bimetallic Pd-Pt catalysts on an Al_2O_3-TiO_2 support. The incorporation of metals was performed using different methods including conventional wet impregnation (IMP), single MOCVD, and a combination of the wet impregnation and MOCVD methods (IMP-MOCVD). The product selectivity of dibenzothiophene hydrodesulfurization was modified by the physicochemical properties of the bimetallic Pd-Pt/Al_2O_3-TiO_2 catalysts, which were influenced by the metal incorporation method. In this report, we try to explain the HDS catalytic activity as a function of the reducibility or hydrogenating properties and the particle size of the bimetallic catalysts.

2. Experimental Procedure

2.1. Support and Catalysts Preparation. The Al_2O_3-TiO_2 support was prepared by the sol-gel method following a previously published procedure [27] using 15 wt.% TiO_2 in the mixed oxide followed by annealing at 500°C. Supported monometallic Pd and Pt catalysts were prepared by either the IMP method or the MOCVD method. In the first metal incorporation method, palladium (II) nitrate dihydrate $Pd[(NO_3)_2{\cdot}2H_2O]$ and tetraammineplatinum (II) nitrate $[Pt(NO_3)_2(NH_3)_4]$ were used as the metallic precursors. A proper solution concentration was used to achieve 1 wt.% Pd and 0.5 wt.% Pt in the final catalysts. The metal incorporation was performed using incipient wetness impregnation by spraying the Pd or Pt solutions. The single impregnated samples were dried at 120°C for 24 h followed by annealing at 500°C in air for 4 h. These samples were labeled Pd-IMP and Pt-IMP. The second metal incorporation method (i.e., single MOCVD) employed $(CH_3–COCHCO–CH_3)_2Pd$ and $(CH_3–COCHCO–CH_3)_2Pt$ as the metal organic complexes. The catalysts were prepared in a horizontal hot-wall type CVD apparatus using the proper quantities of the support and metal precursor to obtain 1.5 wt.% Pd and 0.5 wt.% Pt the monometallic Pd and Pt catalysts. Each metallic precursor (i.e., Pd or Pt) was separately evaporated at 180°C. The deposition temperature (T_{dep}) was maintained at 400°C, and the total pressure (P_{tot}) was maintained at 1 Torr. These samples denoted Pd-MOCVD and Pt-MOCVD. The bimetallic Pd-Pt catalysts supported on the Al_2O_3-TiO_2 carrier were prepared by (A) single wet impregnation (IMP), (B) single MOCVD, and (C) a combined Pd-IMP/Pt-MOCVD method, and the resulting catalysts were labeled Pd-Pt-IMP, Pd-Pt-MOCVD, and Pd-IMP/Pt-MOCVD, respectively. A nominal loading of 1 wt.% Pd and 0.5 wt.% Pt was used for all of the catalysts. The bimetallic Pd-Pt-IMP catalyst was prepared by wet impregnation of the Al_2O_3-TiO_2 using the same palladium (II) and platinum (II) solutions. The wet catalyst was dried and annealed as mentioned above for the monometallic catalysts. The bimetallic Pd-Pt-MOCVD catalyst was prepared using proper amounts of both $Pd(acac)_2$ and $Pt(acac)_2$ precursors, which were evaporated together at 180°C followed by drying and annealing according to the abovementioned conditions. The preparation of bimetallic catalyst Pd-IMP/Pt-MOCVD was carried out in two steps. First, the Pd was incorporated using the IMP method with an aqueous solution of palladium (II) nitrate, and then the Pt was integrated using the MOCVD method to yield Pd-IMP/Pt-MOCVD.

2.2. Support and Catalysts Characterization. Characterizations of the alumina-titania support, the monometallic IMP and MOCVD catalysts, and the bimetallic IMP, MOCVD, and IMP/MOCVD catalysts were performed. Additional characterization of Pd-MOCVD, Pt-MOCVD, and Pd-Pt-MOCVD was performed for the freshly prepared samples.

2.2.1. Textural Properties of the Al_2O_3-TiO_2 Support. Textural properties of the support were determined by N_2 physisorption at 77 K with a Micromeritics ASAP-2000 apparatus. Surface areas and pore size distributions were calculated using the BET and desorption BJH methods, respectively.

2.2.2. XRD and Raman Spectroscopy. Powder X-ray diffraction (XRD) of the alumina-titania support was performed on a Siemens D8 focus diffractometer with Cu Kα radiation (α = 0.15406 nm). The Raman spectra of the alumina-titania support were obtained at room temperature using a Horiba Jobin Yvon Inc. T64000 spectrometer equipped with a confocal microscope (Olympus BX41) with a 514.5 nm line generated by an Ar^+ laser (5 mW).

2.2.3. Temperature Programmed Reduction (TPR). Temperature programmed reduction (H_2-TPR) of catalysts previously annealed at 500°C was conducted with Altamira AMI200 TPR equipment. The experiments were performed in a quartz reactor coupled to a thermal conductivity detector (TCD), and the reduction stream included an H_2 (10%vol)/argon certified mixture. 50 mg of each sample was reduced from 273 to 1123 K by passing the gas mixture at a flow rate of 30 mL/min (10°K/min was the heating rate).

2.2.4. High Resolution Transmission Electron Microscopy (HRTEM). High resolution transmission electron microscopy (HRTEM) was performed with an FEI Tecnai 20 instrument at a point resolution of 1.7 Å and an acceleration voltage of 200 keV. The samples of the monometallic and bimetallic Pd and Pt catalysts (fresh, sulfided, and spent) were suspended in acetone. One droplet of the suspension was applied to a 400-mesh carbon-coated copper grid and left to dry in air.

2.3. Catalytic Evaluation of the HDS of DBT. Prior to the catalytic evaluation, all of the catalysts were heated at 400°C in an N_2 atmosphere and then sulfided *in situ* by flowing a 10% H_2S/H_2 gas mixture at 400°C for 1 h. Next, catalyst activation was tested for the HDS of DBT in a stirred batch reactor (Parr 4562 M). The reaction mixture was prepared by dissolving ~0.3 g of Aldrich DBT in 100 cm^3 of Aldrich *n*-hexadecane (98 wt-% and 99 wt-% purity, resp.) followed by the addition of 200 mg of sieved catalyst (80–100 Tyler mesh, 0.165 mm average particle diameter). The operating conditions, which were carefully chosen to avoid external and/or internal diffusion limitations, were $P = 5.59 \pm 0.03$ MPa, $T = 350 \pm 2$°C, and 1000 rpm (~105 rad s^{-1}) mixing speed. Samples were periodically (1, 2, 3, and 4 h) analyzed in a gas chromatograph Perkin-Elmer AutoSystem XL (flame ionization detector and column Econo-CAP5 from Alltech). HDS kinetic constants were estimated assuming pseudo-first-order kinetics referred to the DBT concentration.

3. Results and Discussion

3.1. Al_2O_3-TiO_2 Support. The BET specific surface area and average pore volume of the mixed oxide Al_2O_3-TiO_2 support were 275 $m^2 g^{-1}$ and 0.76 $cm^3 g^{-1}$, respectively. In addition, the mean pore diameter was 110 Å. The X-ray diffraction analysis (not shown) of the Al_2O_3-TiO_2 support indicated the presence of well-crystallized γ-Al_2O_3 and signals corresponding to crystalline TiO_2 in the anatase phase. The appearance of the signal corresponding to the anatase phase suggested that it is well crystallized and segregated with TiO_2 domains [21]. The laser Raman spectra of the support exhibited (not shown) signals corresponding to the anatase phase that were shifted to 395, 517, and 637 cm^{-1} [28, 29].

3.2. Temperature Programmed Reduction (TPR) of the Monometallic and Bimetallic Catalysts. Figure 1 shows the TPR of the monometallic oxide (Pd and Pt catalysts) incorporated on the Al_2O_3-TiO_2 support by the IMP method. The monometallic Pd-IMP catalyst was reduced from room temperature to 850°C. In addition, the negative profiles correspond to palladium hydride (Pd-H_x) formation at 102°C, and some changes of these types of sites were observed at 381 and 616°C (Figure 1). For the reduction profile, the PdO over Al_2O_3 is immediately reduced at 30°C but when PdO is deposited on TiO_2, it is expected to be reduced below 0°C (not shown). The absence of reduction peaks at room temperature suggests that PdO could be deposited onto the TiO_2 rich matrix. However, unimportant

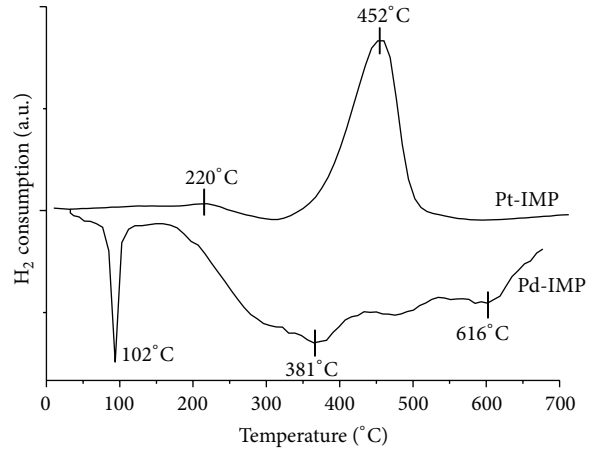

Figure 1: H_2-TPR spectra of Al_2O_3-TiO_2 supported monometallic Pt-IMP and Pd-IMP catalysts.

variations in the temperature of the Pd-H_x formation were observed when Ti^{4+} is present in the Al_2O_3 matrix, as reported by Wang et al. [30]. However, the temperature of this event was higher than that reported for the Pd-H_x formation on Al_2O_3 (80°C) and Al_2O_3-TiO_2 (75°C). This increase in the temperature could be associated with the strong interaction between PdO and the Al_2O_3-TiO_2 support. In addition, the high intensity of the main peak (i.e., Pd-H_x) suggests low dispersion of the Pd particles in this catalyst [23, 31].

The TPR of the monometallic Pt-IMP catalyst exhibits a first reduction peak at 220°C, which corresponds to the reduction of the Pt^{2+} species to Pt^0 due to interaction with Al_2O_3. The PtO reduction on Al_2O_3 has been reported at 220–250°C [32, 33]. In addition, the second reduction peak was observed at 460°C due to the partial reduction of TiO_2 by hydrogen with the metal-support interaction (MSI), which has been reported to occur in the range of 360–600°C [34]. This H_2 consumption peak for Pt/TiO_2 is shifted to a higher temperature, which implies a strong metal-support interaction (SMSI) between Pt and the TiO_2 rich matrix. This result is associated with the reduction of TiO_2 promoted by the presence of Pt, which suggested that Pt is preferentially deposited onto the TiO_2 rich matrix and only a small amount of Pt is deposited on the Al_2O_3 surface.

The TPR profiles of the bimetallic Pd-Pt-IMP, Pd-Pt-MOCVD, and Pd-IMP/Pt-MOCVD catalysts are shown in Figure 2. The TPR profiles contain only a few peaks including a positive peak and a negative one for all of the samples. The first peak appears at 25°C due to PdO reduction of Pd^{+2} to Pd^0, and the second peak was observed at 67–97°C due to the Pd-H_x formation on the Pd crystallites [31]. Based on the analysis of the TPR profile of the bimetallic Pd-Pt catalysts, we can assume that they are not a simple sum of the monometallic samples. Apparently, the Pd and Pt particles coexist in close proximity, which can be deduced from the shift in the peak corresponding to the Pd-H_x formation. The decrease in the formation of Pd-H_x is influenced not only by the dispersion of Pd particles but also by the Pt content in the Pd-Pt alloy [31]. In our case, the negative

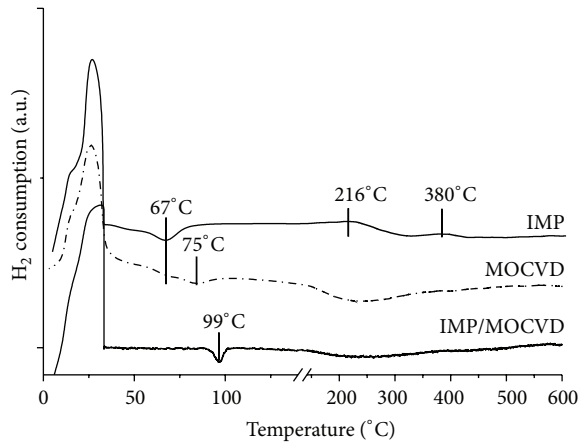

Figure 2: Reduction profiles of bimetallic Pd-Pt catalysts prepared by (a) IMP, (b) MOCVD, and (c) IMP/MOCVD method.

peak of the Pd-H_x formation for the three bimetallic catalysts appears at different temperature. For the IMP catalysts, the negative peak appears at 67°C, and for the MOCVD catalysts, the negative peak appears at 75°C with a shoulder at 67°C. For the IMP/MOCVD catalyst, the negative peak appears at 99°C, which suggests that part of the deposited Pd particles in the bimetallic Pd-Pt catalysts is present either as isolated metal particles with low dispersion or alloyed with Pt. For both bimetallic IMP and MOCVD catalysts, the peak corresponding to the Pd-H_x formation is in agreement with that reported by Baldovino-Medrano et al. [35], where the interaction between Pd and Pt modifies the temperature of the Pd-H_x formation to 63°C. Navarro et al. [16] detected a broad peak at 379°C, which was due to the reduction of the Pd particle along with the coimpregnated Pt particles resulting from an interaction between them. However, in our case, these interactions are present only in the IMP catalysts.

Only the bimetallic Pd-Pt-IMP catalyst exhibited reduced PtO on Al_2O_3 at 216°C. In the remaining catalysts prepared by the MOCVD method, this reduction was not observed, which suggests that when the Pt is incorporated with the MOCVD method using an organometallic precursor, the Pt could be present as elemental platinum (Pt^0), as was reported by Stakheev and Kustov [36]. In addition, for the bimetallic IMP/MOCVD catalyst, the presence of Pt^0 slightly modifies the nature of the PdO crystalline particles previously deposited by the IMP method leading to species with a different nature, which results in the slight shift in the peak corresponding to Pd-H_x formation (99°C). However, the temperature of its formation is similar to that of the monometallic Pd-IMP catalyst (102°C, see Figure 1), which indicates the presence of poorly dispersed Pd particles that can influence the activity and selectivity of the HDS of DBT.

For all of the bimetallic catalysts, the Al_2O_3-TiO_2 support did not exhibit an H_2 consumption signal at high temperatures (400–600°C), which indicated that the partial reduction of Ti^{4+} to Ti^{3+} did not occur after Pt incorporation [34]. This result is not surprising for the bimetallic MOCVD and IMP/MOCVD catalysts because the MOCVD method affords Pt^0 species, which prevent the strong metal-support interaction (SMSI) between PtO and the TiO_2 matrix. By contrast, for the bimetallic IMP catalysts, the PtO particles are most likely formed only on the Al_2O_3 matrix.

3.3. High Resolution Transmission Electron Microscopy

3.3.1. HRTEM of the Freshly Prepared Monometallic Pd and Pt Alumina-Titania Catalysts. Figures 3(a)–3(d) show the HRTEM images of the Pd and Pt catalysts prepared using the different incorporation methods. Micrograph images revealed that the support contains monometallic nanoparticles of Pd and Pt. The nanoparticles are preferentially formed near or over the nanocrystallites of the well-dispersed TiO_2 in the network. For TiO_2 dispersion of this type of material, we have demonstrated by TEM that the presence of very small TiO_2 particles in the support is homogeneously dispersed over and inside the alumina matrix, which facilitates the formation of more active metallic phases [27]. A predominant unimodal size distribution varying from 5 to 10 nm was observed for the monometallic Pd and Pt particles incorporated using the impregnation (IMP) method. However, these particles tend to agglomerate, which resulted in the low dispersion of the metallic particles as indicated by the TPR study. By contrast, when the metal incorporation was performed with the MOCVD method, the monometallic catalysts exhibited good dispersion and homogeneity of the small metallic particles on the Al_2O_3-TiO_2 support. The main difference is the presence of a bimodal size distribution with particles varying in size from 5 to 8 nm with an average particle size of 2–5 nm. In both cases, these monometallic particles are preferentially formed near the crystallites of TiO_2 present in the network, as indicated by the TPR results.

3.3.2. HRTEM of the Freshly Prepared Bimetallic Pd-Pt Catalysts. More information regarding the particle size of both the Pd and Pt particles over the Al_2O_3-TiO_2 support could be determined using HRTEM characterization of the bimetallic catalysts. Figures 4(a)–4(c) show the HRTEM micrographs of the bimetallic Pd-Pt-IMP, Pd-Pt-MOCVD, and Pd-IMP/Pt-MOCVD catalysts. From numerous HRTEM micrographs, histograms of the particle size distribution were obtained for the three catalysts. It is important to note that, due to the low metal loading, the particles are difficult to observe in most areas, and these particles are inhomogeneously distributed. Therefore, Figures 4(a)–4(c) are not typical of the overall distribution but instead represent an area with a particular nanoparticles density. Figures 4(a)–4(c) show the influence of the incorporation method on the crystallite size of the bimetallic Pd-Pt catalysts. A predominant unimodal size distribution varying from 5 to 10 nm was observed for the codeposited Pd-Pt particles incorporated by either the single impregnation or MOCVD method. However, there are differences in the size of the bimetallic particles depending on the method of preparation, and although the sample of Pd-Pt obtained by impregnation shows small crystallites with an average size of 5–8 nm, there are some regions where crystallites tend to form agglomerates.

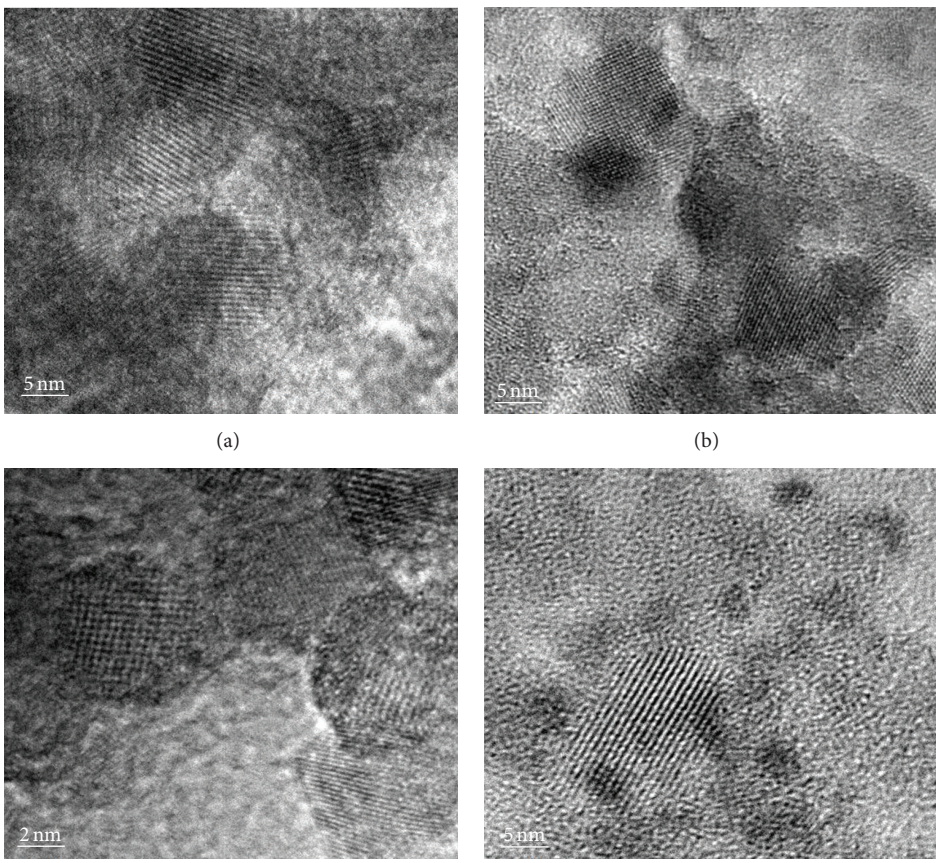

(a) (b)

(c) (d)

Figure 3: HRTEM images of the Pd and Pt catalysts prepared by IMP and MOCVD methods. (a) Pd-IMP, (b) Pd-MOCVD, (c) Pt-IMP, and (d) Pt-MOCVD catalysts.

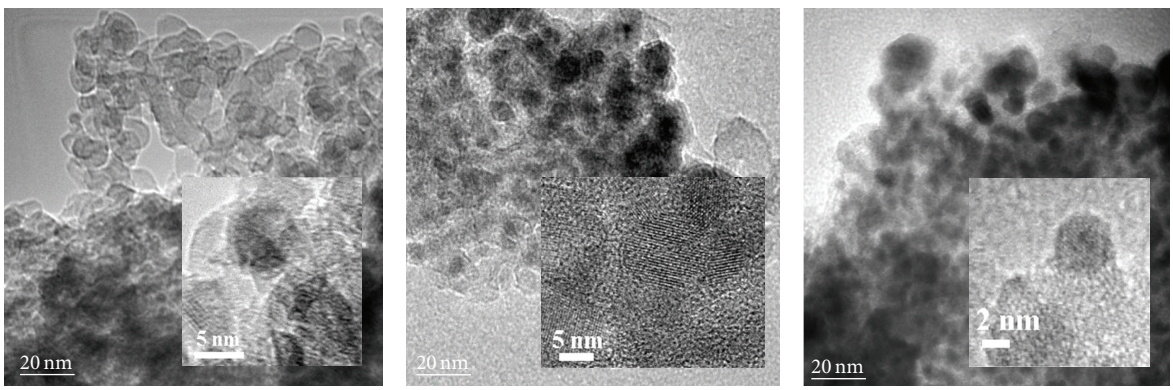

(a) (b) (c)

Figure 4: HRTEM micrographs of the three Pd-Pt catalysts prepared by different method. (a) Impregnation, (b) MOCVD, and (c) Impregnation/MOCVD.

The Pd-IMP/Pt-MOCVD catalyst exhibits a bimodal size distribution of particles. Figures 4(a)–4(c) also indicate the presence of a significant amount of smaller particles varying from 2 to 4 nm on the previously formed Pd particles. The uniform dispersion observed in the catalyst prepared using the MOCVD method was not affected by the combination of methods in the synthesis of the bimetallic IMP/MOCVD catalyst because the particles on the support are very similar to that observed in the monometallic sample. The integration of Pd using the IMP method with subsequent incorporation of Pt by the MOCVD method prevents the formation of large crystallites of Pt^0 on the Al_2O_3-TiO_2 surface and favors

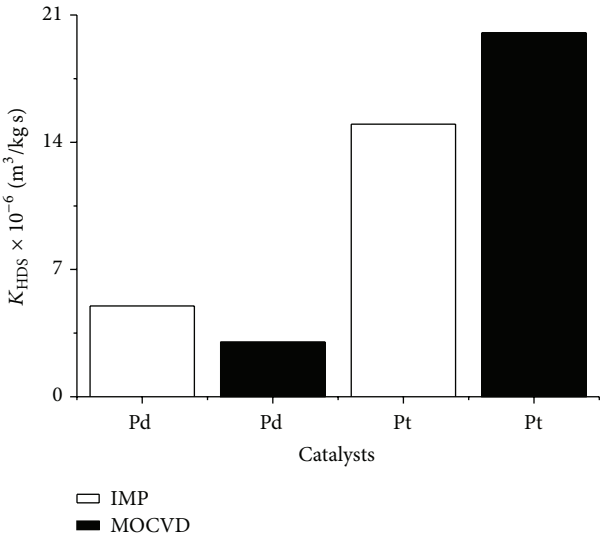

Figure 5: Pseudo-first-order HDS intrinsic kinetic constants over monometallic Pt and Pd catalysts (P = 5.59 MPa, T = 350°C).

the growth of smaller Pt^0 crystallites on previous and larger impregnated PdO particle, which could account for the increase in the activity for HDS.

3.4. HDS of DBT over the Monometallic Catalysts. Figure 5 shows the DBT hydrodesulfurization rate constants of the monometallic catalysts. The most active catalyst was Pt/Al_2O_3-TiO_2, especially when prepared using the MOCVD method. In both cases, the low metallic content (0.5% wt.) allows for a high dispersion of Pt on the TiO_2 matrix, and the interactions between Pt and TiO_2 may be responsible for the high catalytic activity that was observed, which is in agreement with the report published by Galindo and de los Reyes [20] and Baldovino-Medrano et al. [35]. The opposite effect was observed for the monometallic Pd catalysts where better catalytic behavior was obtained over the Pd-IMP catalyst. In this particular case, the low HDS activity of both the Pd-IMP and Pd-MOCVD catalysts may be associated with the low dispersion of the Pd particles.

3.4.1. Selectivity of the Monometallic Catalysts. The product reaction species observed in the HDS of DBT over the monometallic Pd and Pt catalysts included biphenyl (BP) as the direct desulfurization product as well as tetrahydrodibenzothiophene (TH-DBT) and cyclohexylbenzene (CHB) as the intermediate and final products of the hydrogenation route, respectively.

Figures 6(a)-6(b) show the selectivity profiles for the HDS of DBT over the monometallic Pd catalysts prepared using the IMP and MOCVD method. The HDS of DBT with the Pd catalyst exhibited significant differences in the mechanism pathway depending on the Pd incorporation method. When the Pd was incorporated with the IMP method, a tendency to form THDBT and CHB products was observed (46% and 17%, resp.). In this case, the low selectivity towards the BP product (36%) at the end of reaction suggests that the hydrogenation route (HYD) proceeds more rapidly than the C–S bond breaking (DDS route), which indicates the presence of Pd hydrogenation sites over the monometallic Pd-IMP. According to Baldovino-Medrano et al. [35], the high selectivity towards products in the HYD route over Pd is associated with a stronger interaction of the aromatics with the Pd active phase and with a lower rate of atomic H transfer from the metal to these rings.

By contrast, the amount of products formed (i.e., THDBT and BP products (50%)) in the HDS of DBT using the monometallic Pd-MOCVD catalyst (Figure 6(b)) was the same as the amount produced in the first hour of the reaction. However, as the reaction progressed, the selectivity of the products evolved resulting in a 6% selectivity for THDBT at the end of the evaluation. In addition, this Pd-MOCVD catalyst exhibited less catalytic activity than the analogous one obtained using the IMP method. The most important feature is the dramatic increase in the presence of BP (94%) with a concomitant disappearance of the THDBT and CHB products. Therefore, once formed, THDBT is dehydrogenated due to the reversibility of the reaction leading to the reformation of DBT, which is eventually desulfurized by the direct mechanism. The hydrogenation/dehydrogenation is faster than the desulfurization route in the HDS of dibenzothiophene over the Pd-γ-Al_2O_3 catalyst at temperatures of 290–330°C [35]. Because our tests were performed at 350°C, the dehydrogenation route may be taking place, which may explain the absence of CHB due to the reversibility of the reaction.

The HDS of DBT with the monometallic Pt catalysts prepared by either the IMP or MOCVD method exhibited a similar catalytic selectivity (Figure 7). The Pt-IMP catalyst exhibited a higher selectivity for the formation of BP (93%) compared to CHB (3%), which confirms a higher C–S bond hydrogenolysis activity (DDS route). The Pt-MOCVD catalyst exhibited a slightly different behavior to that observed for the Pt-IMP catalyst. In this case, the presence of THDBT (approximately 14%) after 1 hour of reaction is slightly higher compared to the analogous catalyst obtained using the IMP method. In addition, the selectivity to BP was approximately 86%. However, at 4 hours of reaction, the selectivity to BP reached 93%, and the presence of the intermediates of the HYD route precursors decreased to less than 7%, which is very similar to that observed for the Pt-IMP catalyst. Therefore, the high selectivity towards BP indicated that the DDS route is more favorable than the HYD route, which is consistent with the previously reported results [1, 23].

3.5. HDS of DBT over the Bimetallic Catalysts. Figure 8(a) shows the kinetic constants for the HDS of DBT after four hours of reaction for both bimetallic catalysts obtained using either the single IMP or MOCVD method, which indicates that the HDS activity of both bimetallic catalysts is nearly the same. Although the bimetallic Pd-Pt-MOCVD catalyst is slightly more active than the Pd-Pt-IMP catalyst, both catalysts exhibit a lower activity than the monometallic Pt catalysts (Figure 5). This low HDS activity may be due to an inhibitor effect of Pd on Pt or to the HDS reaction being strongly influenced by the presence of Pd.

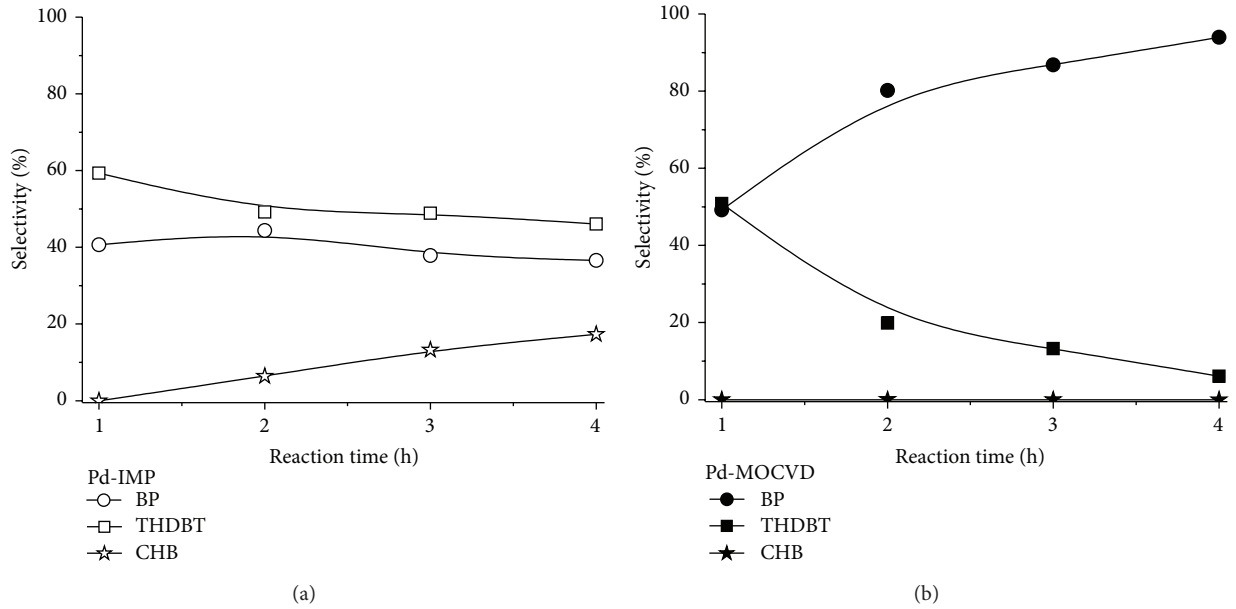

Figure 6: Profiles of HDS selectivity in the HDS of DBT reaction over monometallic Pd catalysts prepared by (a) IMP and (b) MOCVD method.

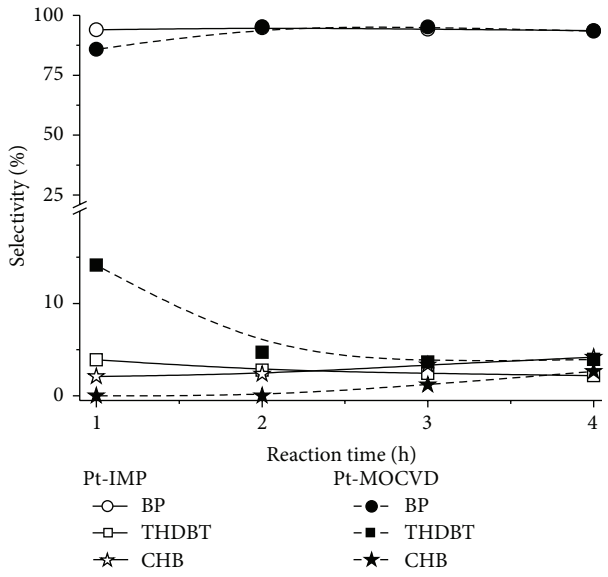

Figure 7: Profiles of HDS selectivity over monometallic Pt catalysts evaluated in the HDS of DBT.

3.5.1. Selectivity of the Pd-Pt Bimetallic Catalyst for the HDS of DBT. The product reaction species observed in the HDS of DBT over the bimetallic Pd-Pt catalysts included biphenyl (BP) as the direct desulfurization product as well as tetrahydrodibenzothiophene (TH-DBT) and cyclohexylbenzene (CHB) as the intermediate and final product of the hydrogenation route, respectively. These products are similar to those obtained from the monometallic Pt catalysts. The Pd-Pt-IMP catalyst did not exhibit significant differences during the evaluation period (Figure 8(b)). After one hour of reaction, this catalyst exhibited selectivity toward the formation of BP, which reached 93%. However, the formation of prehydrogenated derivatives was less than 7%. The presence of BP remained constant irrespectively of the reaction time. Based on these results, the selectivity of the products was influenced by the presence of the Pt species on the support surface. As observed for the monometallic Pt catalyst (Figure 7), desulfurized products were obtained, which has been previously reported [1, 15, 23].

The bimetallic Pd-Pt-MOCVD catalyst exhibited a slightly different trend compared to that observed for the catalyst prepared using the single IMP method. Surprisingly, the Pd-Pt-MOCVD catalyst only produced BP and THDBT without the formation of CHB (Figure 8(b)), which indicates that, for this particular catalyst, the subsequent hydrogenation step of THDBT is rate determining. This result is similar to that observed for the monometallic Pd-MOCVD catalyst. Here, the selectivity may be associated with the presence of isolated Pd species. As proposed by Houalla et al. [7], the reaction pathways for the HDS of DBT are the direct desulfurization to BP and hydrogenation to yield THDBT or HHDBT, which are further desulfurized to CHB. In our case, the formation of HHDBT was not detected with the Pd-Pt-MOCVD catalyst. In addition, for this catalyst, only the formation of BP was observed, which may be result from direct desulfurization as well as dehydrogenation of THDBT due to the ability of Pd to dehydrogenate these types of rings [35]. The Pd/(Pd + Pt) molar ratio can modify the competition between the hydrogenation-dehydrogenation C–S–C bond scission reactions occurring during the HDS of DBT, which indicates that the optimal molar ratio is (0.8) for Pd-Pt deposited on Al_2O_3. In addition, bimetallic Pd-Pt/Al_2O_3 prepared from nitrate or organometallic precursors possesses a higher DDS selectivity than those prepared from

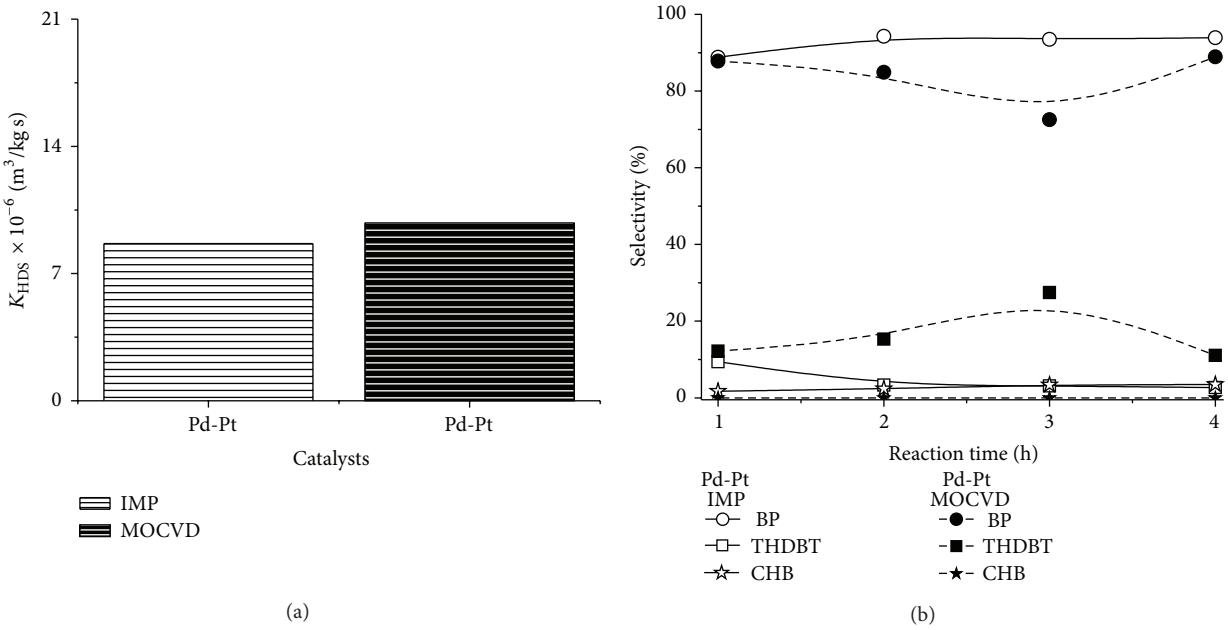

Figure 8: (a) Pseudo-first-order HDS intrinsic kinetic constants and (b) profile of HDS selectivity over bimetallic Pd-Pt catalysts evaluated in the HDS of DBT (P = 5.59 MPa, T = 350°C).

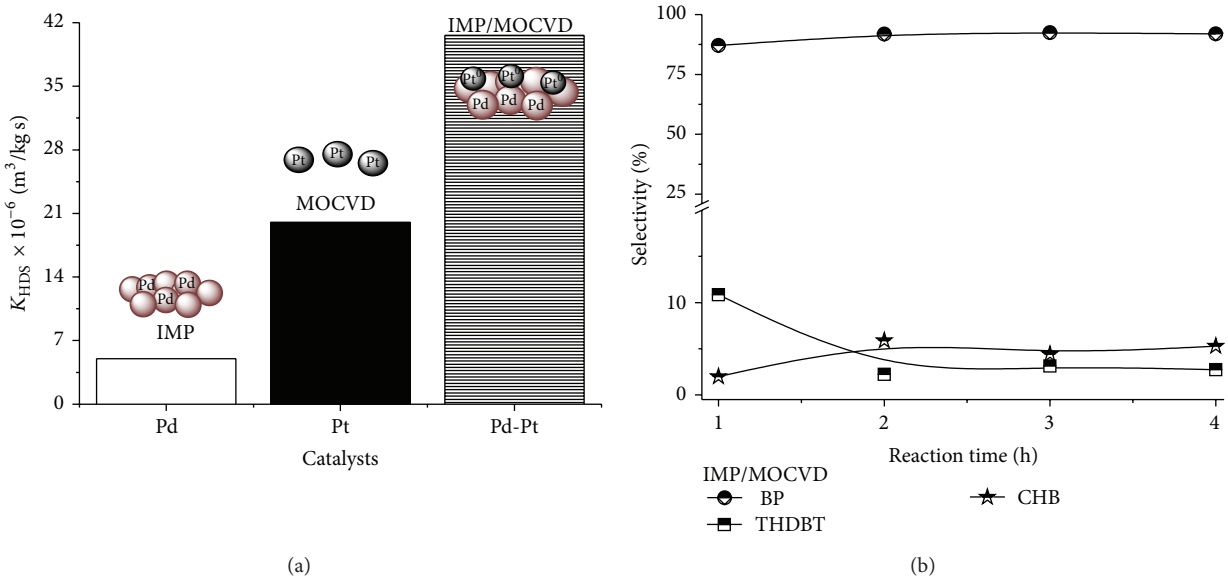

Figure 9: (a) Pseudo-first-order HDS intrinsic kinetic constants over Pd-IMP, Pt-MOCVD, and Pd-Pt-IMP/MOCVD catalysts evaluated in the HDS of DBT and (b) profiles of HDS selectivity over Pd-Pt-IMP/MOCVD catalysts (P = 5.59 MPa, T = 350°C).

chloride precursors [35]. In our case, the bimetallic Pd-Pt supported on Al_2O_3-TiO_2 exhibited DDS selectivity because the Pd/(Pd + Pt) molar ratio (0.75) was close to the optimal value and they were incorporated from organometallic precursors.

3.6. HDS Activity of DBT with the Bimetallic IMP/MOCVD Catalyst. Because the monometallic Pd-IMP and Pt-MOCVD catalysts exhibited individually high HDS activity, we prepared a bimetallic Pd-Pt catalyst by combining the IMP and MOCVD methods. Figure 9(a) shows the kinetic constants for the HDS of DBT for the bimetallic catalysts compared to their respective monometallic catalysts (i.e., Pd-IMP and Pt-MOCVD). After four hours of reaction, the HDS activity of the Pd-IMP/Pt-MOCVD catalyst was twice as high as that of the monometallic Pt-MOCVD catalyst, which indicated that a synergic effect was achieved due to the interaction of the Pd particles over TiO_2 matrix when both Pd and Pt particles were incorporated using a combination of the IMP and MOCVD method, respectively. In addition, the HDS activity of the better bimetallic catalyst was four times higher than that obtained from the catalysts

prepared with either the single IMP or MOCVD method (Figure 8(a)), which indicated that the catalytic activity was strongly improved when Pt^0 is dispersed or deposited on the PdO particles that were previously incorporated onto the Al_2O_3-TiO_2 support rather than being incorporated in one step. This result indicates that the HDS activity of the bimetallic catalyst was influenced by the metal incorporation methods.

3.6.1. Selectivity of Pd-Pt-IMP/MOCVD for the HDS of DBT. The results in Figure 9(b) show that the selectivity results of this catalyst closely resemble the trend observed for the bimetallic Pd-Pt-IMP catalysts. At a shorter reaction time (1 hour), significant amounts of intermediate prehydrogenated products were detected. However, the selectivity towards BP reached 87%, but after 2 hours of reaction the selectivity increased to 91% for BP and ~3 and ~5% for THDBT and CHB, respectively. Then, these values remained constant. This behavior suggests that the HDS selectivity was influenced by the presence of Pt dispersed on either the PdO or TiO_2 rich matrix surface.

4. Conclusions

In this study, we synthesized Al_2O_3-TiO_2 supported bimetallic Pd-Pt catalysts prepared using a single IMP, single MOCVD, and combined IMP/MOCVD methods. The most active bimetallic catalyst for the HDS of DBT was the catalyst prepared using the combined IMP/MOCVD method. This HDS activity of this catalyst was four times higher than that obtained with catalysts prepared using the single IMP or MOCVD methods. Based on the observed selectivity, all of the catalysts exhibited a preference for the removal of sulfur via direct desulfurization. However, the single MOCVD method does not considerably improve the activity of HDS of DBT but influences the selectivity where the reversibility of the reaction appears to favor the direct desulfurization pathway, which is the preferred mechanism in the DBT reaction. The TPR and TEM results indicated that the incorporation of active noble metals by combining techniques influences the particle size and dispersion of Pt over the Pd particles and may be responsible for improving the catalytic activity for the HDS of DBT.

Conflict of Interests

The authors declare that there is no conflict of interests regarding the publication of this paper.

Acknowledgments

The authors wish to acknowledge the financial support from the National Polytechnic Institute (SIP-20144667 and SIP-20140106); and ICYTDF (45/2012). R. Martínez Guerrero wishes to thank the IPN and CONACYT for financial support of his doctoral studies.

References

[1] http://epa.gov/OTAQ/fuels/dieselfuels/index.htm.

[2] A. Stanislaus, A. Marafi, and M. S. Rana, "Recent advances in the science and technology of ultra low sulfur diesel (ULSD) production," *Catalysis Today*, vol. 153, no. 1-2, pp. 1–68, 2010.

[3] R. Bacaud, V. L. Cebolla, L. Membrado, M. Matt, S. Pessayre, and E. M. Gàlvez, "Evolution of sulfur compounds and hydrocarbons classes in diesel fuels during hydrodesulfurization. Combined use of thin-layer chromatography and GC-sulfur-selective chemiluminescence detection," *Industrial & Engineering Chemistry Research*, vol. 41, no. 24, pp. 6005–6014, 2002.

[4] F. Bataille, J.-L. Lemberton, P. Michaud et al., "Alkyldibenzothiophenes hydrodesulfurization-promoter effect, reactivity, and reaction mechanism," *Journal of Catalysis*, vol. 191, no. 2, pp. 409–422, 2000.

[5] C. Song and X. Ma, "New design approaches to ultra-clean diesel fuels by deep desulfurization and deep dearomatization," *Applied Catalysis B: Environmental*, vol. 41, no. 1-2, pp. 207–238, 2003.

[6] R. Shafi and G. J. Hutchings, "Hydrodesulfurization of hindered dibenzothiophenes: an overview," *Catalysis Today*, vol. 59, no. 3-4, pp. 423–442, 2000.

[7] M. Houalla, N. K. Nag, A. V. Sapre, D. H. Broderick, and B. C. Gates, "Hydrodesulfurization of dibenzothiophene catalyzed by sulfided CoO-MoO_3 γ-Al_2O_3: the reaction network," *AIChE Journal*, vol. 24, no. 6, pp. 1015–1021, 1978.

[8] M. Houalla, D. H. Broderick, A. V. Sapre et al., "Hydrodesulfurization of methyl-substituted dibenzothiophenes catalyzed by sulfided Co-Mo γ-Al_2O_3," *Journal of Catalysis*, vol. 61, no. 2, pp. 523–527, 1980.

[9] Y. Yoshimura, M. Toba, H. Farag, and K. Sakanishi, "Ultra deep hydrodesulfurization of gas oils over sulfide and/or noble metal catalysts," *Catalysis Surveys from Asia*, vol. 8, no. 1, pp. 47–60, 2004.

[10] J. M. Thomas and W. J. Thomas, *Principles and Practice of Heterogeneous Catalysis*, VCH, New York, NY, USA, 1997.

[11] G. Ertl, H. Knözinger, and J. Weitkamp, Eds., *Handbook of Heterogeneous Catalysis*, Wiley-VCH, New York, NY, USA, 1997.

[12] A. Niquille-Röthlisberger and R. Prins, "Hydrodesulfurization of 4,6-dimethyldibenzothiophene and dibenzothiophene over alumina-supported Pt, Pd, and Pt-Pd catalysts," *Journal of Catalysis*, vol. 242, no. 1, pp. 207–216, 2006.

[13] A. Ishihara, F. Dumeignil, J. Lee, K. Mitsuhashi, E. W. Qian, and T. Kabe, "Hydrodesulfurization of sulfur-containing polyaromatic compounds in light gas oil using noble metal catalysts," *Applied Catalysis A: General*, vol. 289, no. 2, pp. 163–173, 2005.

[14] A. Yasuda and Y. Yoshimura, "Hydrogenation of tetralin over zeolite-supported Pd-Pt catalysts in the presence of dibenzothiophene," *Catalysis Letters*, vol. 46, no. 1-2, pp. 43–48, 1997.

[15] A. Niquille-Röthlisberger and R. Prins, "Hydrodesulfurization of 4,6-dimethyldibenzothiophene over Pt, Pd, and Pt-Pd catalysts supported on amorphous silica-alumina," *Catalysis Today*, vol. 123, no. 1–4, pp. 198–207, 2007.

[16] R. M. Navarro, B. Pawelec, J. M. Trejo, R. Mariscal, and J. L. G. Fierro, "Hydrogenation of aromatics on sulfur-resistant PtPd bimetallic catalysts," *Journal of Catalysis*, vol. 189, no. 1, pp. 184–194, 2000.

[17] A. E. Cordero-Borboa, E. Sterling-Black, A. Gomez-Cortes, and A. Vazquez-Zavala, "X-ray diffraction evidence of the single solid solution character of bi-metallic Pt-Pd catalyst particles

on an amorphous SiO_2 substrate," *Applied Surface Science*, vol. 220, no. 1–4, pp. 169–174, 2003.

[18] H. Jiang, H. Yang, R. Hawkins, and Z. Ring, "Effect of palladium on sulfur resistance in Pt-Pd bimetallic catalysts," *Catalysis Today*, vol. 125, no. 3-4, pp. 282–290, 2007.

[19] C. C. C. Augusto, J. L. Zotin, and A. D. C. Faro Jr., "Effect of sulfur or nitrogen poisoning on the activity and selectivity of Y-zeolite-supported Pt-Pd catalysts in the hydrogenation of tetralin," *Catalysis Letters*, vol. 75, no. 1-2, pp. 37–43, 2001.

[20] I. R. Galindo and J. A. de los Reyes, "Effect of alumina-titania supports on the activity of Pd, Pt and bimetallic Pd-Pt catalysts for hydrorefining applications," *Fuel Processing Technology*, vol. 88, no. 9, pp. 859–863, 2007.

[21] W. Guofu, D. Aijun, Z. Zhen et al., "Al_2O_3-TiO_2/Al_2O_3-TiO_2-SiO_2 composite-supported bimetallic Pt-Pd catalysts for the hydrodearomatization and hydrodesulfurization of diesel fuel," *Energy & Fuels*, vol. 23, no. 1, pp. 81–85, 2009.

[22] J. A. Schwarz, C. Contescu, and A. Contescu, "Methods for preparation of catalytic materials," *Chemical Reviews*, vol. 95, no. 3, pp. 477–510, 1995.

[23] Z. Vít, D. Gulkova, L. Kaluža, and M. Boarob, "Effect of catalyst precursor and its pretreatment on the amount of β-Pd hydride phase and HDS activity of Pd-Pt/silica-alumina," *Applied Catalysis B: Environmental*, vol. 146, pp. 213–220, 2014.

[24] A. E. Aksoylu, J. L. Faria, M. F. R. Pereira et al., "Highly dispersed activated carbon supported platinum catalysts prepared by OMCVD: a comparison with wet impregnated catalysts," *Applied Catalysis A: General*, vol. 243, no. 2, pp. 357–365, 2003.

[25] V. Cominos and A. Gavriilidis, "Preparation of axially non-uniform Pd catalytic monoliths by chemical vapour deposition," *Applied Catalysis A: General*, vol. 210, no. 1-2, pp. 381–390, 2001.

[26] J. R. Vargas Garcia and T. Goto, "Chemical vapor deposition of iridium, platinum, rhodium and palladium," *Materials Transactions*, vol. 44, no. 9, pp. 1717–1728, 2003.

[27] V. Santes, J. Herbert, M. T. Cortez et al., "Catalytic hydrotreating of heavy gasoil FCC feed on alumina–titania-supported NiMo catalysts," *Applied Catalysis A: General*, vol. 281, pp. 121–128, 2005.

[28] I. E. Wachs, "Raman and IR studies of surface metal oxide species on oxide supports: supported metal oxide catalysts," *Catalysis Today*, vol. 27, no. 3-4, pp. 437–455, 1996.

[29] R. Tomaszek, L. Pawlowski, J. Zdanowski, J. Grimblot, and J. Laureyns, "Microstructural transformations of TiO_2, Al_2O_3 + 13TiO_2 and Al_2O_3+ 40TiO_2 at plasma spraying and laser engraving," *Surface and Coatings Technology*, vol. 185, no. 2-3, pp. 137–149, 2004.

[30] C.-B. Wang, H.-K. Lin, and C.-M. Ho, "Effects of the addition of titania on the thermal characterization of alumina-supported palladium," *Journal of Molecular Catalysis A: Chemical*, vol. 180, no. 1-2, pp. 285–291, 2002.

[31] P. Sangeetha, K. Shanthi, K. S. R. Rao, B. Viswanathan, and P. Selvam, "Hydrogenation of nitrobenzene over palladium-supported catalysts—effect of support," *Applied Catalysis A: General*, vol. 353, no. 2, pp. 160–165, 2009.

[32] N. S. De Resende, J.-G. Eon, and M. Schmal, "Pt-TiO_2-γ Al_2O_3: catalyst I. Dispersion of platinum on alumina-grafted titanium oxide," *Journal of Catalysis*, vol. 183, no. 1, pp. 6–13, 1999.

[33] M. Bhagiyalakshmi, R. Anuradha, S. D. Park, T. S. Park, W. S. Cha, and H. T. Jang, "Effect of bimetallic Pt-Rh and trimetallic Pt-Pd-Rh catalysts for low temperature catalytic combustion of methane," *Bulletin of the Korean Chemical Society*, vol. 31, no. 1, pp. 120–124, 2010.

[34] K.-P. Yu, W.-Y. Yu, M.-C. Kuo, Y.-C. Liou, and S.-H. Chien, "Pt/titania-nanotube: a potential catalyst for CO_2 adsorption and hydrogenation," *Applied Catalysis B: Environmental*, vol. 84, pp. 112–118, 2008.

[35] V. G. Baldovino-Medrano, P. Eloy, E. M. Gaigneaux, S. A. Giraldo, and A. Centeno, "Development of the HYD route of hydrodesulfurization of dibenzothiophenes over Pd-Pt/γ-Al_2O_3 catalysts," *Journal of Catalysis*, vol. 267, no. 2, pp. 129–139, 2009.

[36] A. Y. Stakheev and L. M. Kustov, "Effects of the support on the morphology and electronic properties of supported metal clusters: modern concepts and progress in 1990s," *Applied Catalysis A: General*, vol. 188, no. 1-2, pp. 3–35, 1999.